Steady Viscosity of a Polymer/Liquid Crystal Biphasic System

I-Kuan Yang, Wei Yuan Lai

Department of Chemical Engineering Tunghai University, Taichung, Taiwan, Republic of China

Received 24 March 2003; accepted 13 October 20003

ABSTRACT: Steady shear viscosities of blends of poly(butyl acrylate) and cholesteryl oleyl carbonate were studied under a cone and plate fixture. Unique shear behavior was observed for the polymer/low molar mass liquid crystal mixture. The viscosity of the liquid crystal-rich phase increases with polymer content until a maximum is reached. The height of the viscosity maximum decreases with the magnitude of the shear stress and disappears when the stress reaches 200 Pa. Addition of liquid crystal to the polymer-rich phase causes a viscosity reduction, and at higher stress levels, the viscosity reduction becomes more effective with the same amount of liquid crystal addition. The viscosity reduction may be related to the fibril morphology of the liquid crystal and the viscosity maximum can be interpreted by the emulsion effect being counteracted by a viscosity reduction effect. A shear-thickening behavior was observed in the intermediate shear rates for the blends with a volume fraction of poly(butyl acrylate) between 9.4 and 49.8%. This is a novel liquid–liquid system that exhibits a shear thickening behavior. © 2004 Wiley Periodicals, Inc. J Appl Polym Sci 92: 25–30, 2004

Key words: blends; shear; rheology; emulsion; liquid crystals

INTRODUCTION

Emulsions and particle suspensions have been the most interesting systems in rheological studies for decades. For both practical needs in industry and academic interest, a great deal of effort has been devoted to investigating numerous liquid/liquid dispersion systems and an abundance of knowledge has been obtained. The variety of liquid/liquid systems investigated includes Newtonian fluid emulsions,[1–4] polymer blends,[5–7] and Newtonian/viscoelastic fluid systems.[8] Rarely have systems involving low molar mass liquid crystals been investigated. Liquid crystals are unique materials that exhibit both fluidity and crystallinity. Their unique features enable wide use in the display industries. One of the potential techniques that could be useful in large-scale flexible displays is the polymer-dispersed liquid crystal system, which contains liquid crystal droplets dispersed in a polymeric binder. Other types of biphasic systems that involve liquid crystalline materials are liquid crystalline polymer (LCP)/flexible polymer blends, frequently used in the plastics industry to reinforce product mechanical properties or enhance processing ease.[9–11] In LCP/flexible polymer systems, a significant viscosity reduction occurs with the addition of a small amount of LCP. On quite a few occasions, a minimum emerges in the concentration-viscosity curve.[12–14] The viscosity reduction mechanism and the minimum occurrence are still under debate. That debate motivates this study. The purpose of this research was to study the steady viscosity behavior of a blend composed of a polymer and a low molar mass liquid crystal that differentiates from the LCP and flexible polymer systems. This research is a preliminary effort to try to understand the mechanism behind the viscosity reduction by the introduction of LCPs into flexible polymers. Similar to LCPs, the low molar mass liquid crystal was found effective in the viscosity reduction, and conversely, addition of a polymer to the low molar mass liquid crystal causes a normal emulsion effect (i.e., a viscosity increase). A surprising shear thickening behavior occurs within the intermediate shear rate range and a concentration window. As far as we know, it is a novel system that exhibits shear-thickening behavior.

MATERIALS

Figure 1 shows the chemical structure formula of the materials used in this study. Cholesteryl oleyl carbonate (ChOC) (provided by Aldrich Chemical Company, Milwaukee, WI) is a cholesteryl ester as well as a low-mass thermotropic liquid crystal. It is found in a variety of applications such as biosensors, pressure indicators, thermometers, etc. By heating from a low temperature, it shows a phase transition from a smectic C-phase to a cholesteric phase and then another transition to a isotropic phase. Poly(butyl acrylate)

Correspondence to: I-K. Yang (ikyang@mail.thu.edu.tw).

Journal of Applied Polymer Science, Vol. 92, 25–30 (2004)

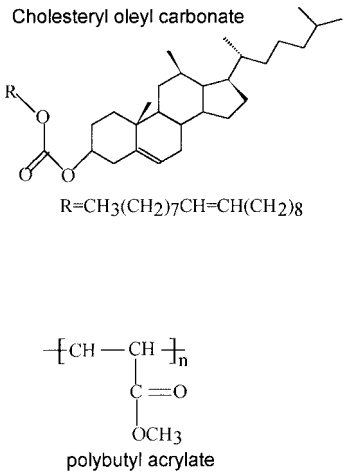

Figure 1 Chemical structures of PBA and ChOC.

(PBA) is a member of polyalkyl acrylates, which shows a glass transition temperature around $-64°C$,[15] and at room temperature it is essentially a viscous fluid.

EXPERIMENTAL

PBA was synthesized by using free-radical polymerization with benzoyl peroxide as the initiator and toluene as the medium. This polymer has a number-average molecular weight of 26,000 and a polydispersity of 6.4. ChOC was supplied by Acros and used directly and its smectic/cholesteric point and cholesteric/isotropic transition point were determined by DSC (Perkin–Elmer Pyris 1) as 20 and 40°C, respectively. The densities of PBA and ChOC were 1.063 and 0.987 g/cm^3. The samples for the rheological measurements were prepared directly by mixing PBA and ChOC at a designated ratio in a beaker with a magnetic stirrer at 45°C for 24 h; the mixture was then cooled to room temperature. It should be noted that at 45°C ChOC is isotropic and at this temperature PBA and ChOC are compatible with limited solubility; ChOC-rich and PBA-rich mixtures at this temperature were found in a homogenous single phase. Cooling down to the room-temperature phase separation was induced. The cooling process controlled the phase morphology of the mixture. By monitoring the phase morphology, it was found that for both ChOC-rich and PBA-rich mixtures that the average size of the droplets increased within the first 5 h after reaching room temperature; then it became stable for another 20 h. Thus, all test samples in the rheological measurements were the stabilized samples. For those samples in the intermediate concentration, there is no way to monitor the size distribution of the droplets because the sample took a bicontinuous morphology. Still, the sample was treated the same way as those having high-ChOC or high-PBA content before rheological measurement. Rheological measurements were performed on a RDA II (Rheometric) with a 50-mm cone and plate fixture at 28°C. At this temperature, ChOC was a cholesteric mesophase according to the DSC phase identification mentioned above. Before each measurement, the loaded sample was allowed to rest for 20 min to relax the strain history formed in the loading procedure. After relaxation, the steady shear viscosities were obtained by using a sequential shear rate stepping up. For each record of the steady viscosity, the sample was allowed to shear under a fixed rate for a sufficient period of time to guarantee that the steady state was reached before stepping up to a higher shear rate. The step-down shearing processes were tested and gave lower viscosities than the stepping-up process because of the slow relaxation process for structure formed under higher shear rates. The viscosity data reported here are all results from the stepping-up measurements. The interfacial tension of PBA/ChOC was determined as 1.6×10^{-4} N/m by measuring the interfacial shape of a tiny ChOC droplet floating on PBA.

RESULTS AND DISCUSSION

As shown in Figure 2, the phase morphologies of the test samples were observed by using cross-polariza-

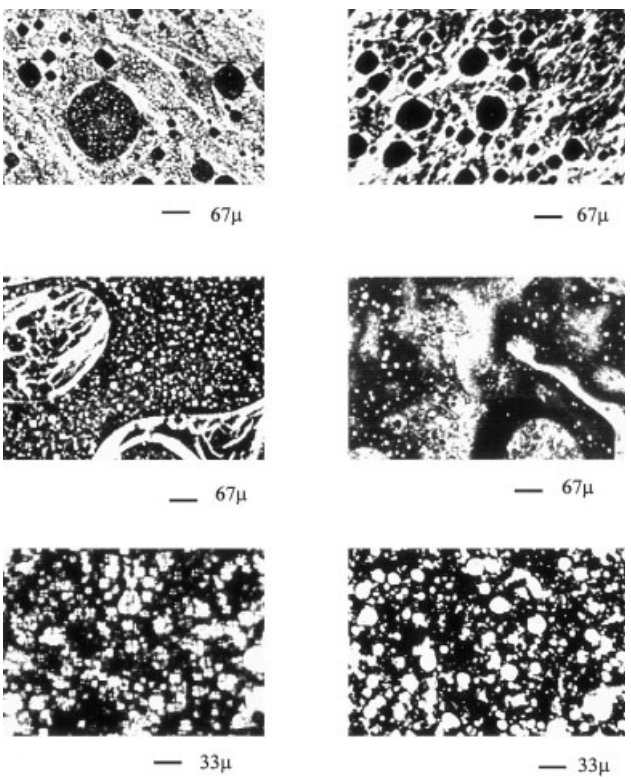

Figure 2 Typical phase morphologies of PBA/ChOC mixtures. Pictures on the left are morphologies before shearing motion and those on the right are after shearing at 10 s^{-1} to steady state. The volume fractions of PBA from top to bottom are 0.28, 0.58, and 0.79, respectively.

tion microscopy before and after the shearing measurement. Before shearing, samples with a PBA volume percentage less than or equal to 28% showed a continuous ChOC phase within which different sized PBA drops were suspended. Large drops were irregular in shape and their diameters were of 60 to 300 μm, estimated by regarding them as spheres. Smaller PBA drops were more spherical in shape and their diameters ranged from 10 to 20 μm. Tiny ChOC droplets that showed a Malta cross under cross polarizers were found inside larger PBA drops. These ChOC droplets were a few micrometers in size. Smaller PBA drops contained no ChOC droplets. In samples whose PBA volume percentages ranged from 38 to 58%, a cocontinuous phase morphology was found. Within continuous ChOC phase, PBA drops could be found, and among those drops, larger ones still duplicated the ChOC droplet inclusion. In continuous PBA phase, ChOC droplets ranging from 2 to 10 μm were suspended. The average size of the suspended droplets in both continuous phases seemed independent of the concentration and only the volume fraction occupied by PBA increased with its content. When the PBA volume percentage reached 68%, the cocontinuous morphology disappeared and PBA occupied the continuous phase in which ChOC drops with diameters ranging from 2 to 20 μm were suspended. After a steady shear at 10 s^{-1}, the sample was immediately put on the stage for microscopic observation. The suspended phase deformation was expected to be completely relaxed from the shearing, and indeed, more spherical droplets were observed than those in irregular shapes. For PBA-rich and ChOC-rich samples, the sizes of the droplets were smaller than those in the same sample before shearing and the inclusion of ChOC droplets in larger PBA drops almost completely disappeared. For samples in bicontinuous morphology, it was essentially impossible to distinguish the morphology before and after shearing, but the disappearance of the ChOC droplet inclusion was noticeable.

Because of its low glass transition temperature, PBA essentially exhibits a Newtonian behavior over the range of shear rate investigated at 28°C, as shown in Figure 3. The shear viscosity of PBA is nearly constant as shear rate increases from 0.01 to 10 s^{-1}. PBA still preserves its elasticity, as one can see from the first normal force difference in Figure 3. PBA, under the measurement conditions, could be regarded as a Newtonian fluid in viscous sense; however, its elasticity might not be negligible.

The rheological behavior of ChOC is completely distinct from PBA in two respects, as shown in Figure 3. First, ChOC is much less viscous than PBA, and second, the former shows shear-thinning behavior throughout shear rate range investigated, although its viscosity tends to level off at higher shear rates. At the

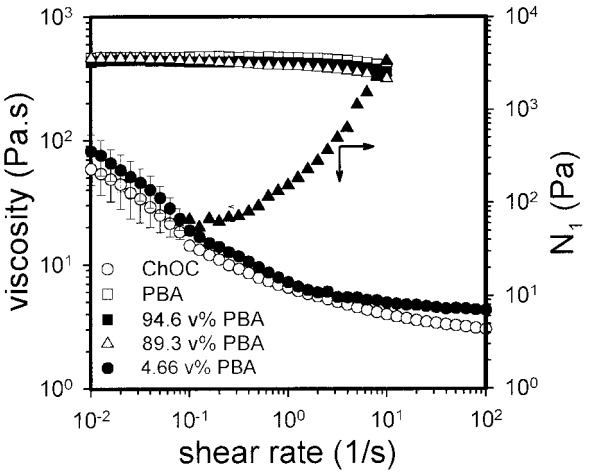

Figure 3 Steady shear viscosities of PBA, ChOC, and low content mixtures.

lowest shear rate, PBA is about 10 times more viscous than ChOC. Because of shear thinning, at higher shear rates, the viscosity ratio of the former to the latter grows to about 200. Shear-thinning behavior has been observed for cholesteric mesophases of both lyotropic[16,17] and thermotropic liquid crystalline materials.[18,19] For a lyotropic solution of hydropropyl cellulose,[16] the shear viscosity versus shear rate curve shows a typical three-region feature as most of the nematic and cholesteric mesophases do.[20] A typical three-region feature consists of a first shear-thinning region at low shear rates followed by a Newtonian plateau in the intermediate rates and a second shear-thinning region at high shear rates. For low mass liquid crystal cholesteric mesophases, the shear-thinning mechanism in the low shear rate region, called region I, is attributed to the persistence of cholestericity[18] in contrast to another mechanism for LCPs involving change in the polydomain structure.[16] A typical three-region feature of a cholesteric liquid crystal system was reported by Pochan and Marsh[19] and interpreted by using a clear picture of the molecular orientation under flow. By using optical measurements, they confirmed that the helical structure of the cholesteric mesophase behaved as a rigid rod tilting with little distortion at low rates. In terms of a dynamic focal-conic texture, or a tilted Grandjean texture and an untilted Grandjean texture, the flow resistance of the sheared mesophase could be explained for shear rates less than 10^3 s^{-1}, which covered the first shear-thinning region and the Newtonian plateau. At shear rates higher than 10^3 s^{-1}, or in the second shear-thinning regime, a homeotropic texture was generated. Our test could not be performed at shear rates higher than 100 s^{-1}, because the centrifugal force pulled the sample out. The data in Figure 3 shows the tendency toward forming a Newtonian plateau as the shear rate approaches 100 s^{-1}. We believe that if mea-

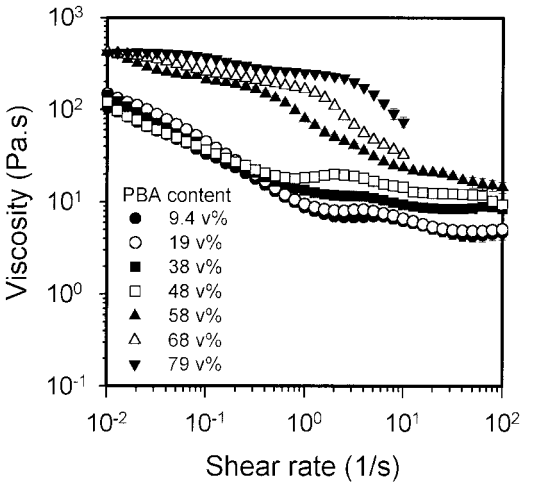

Figure 4 Steady shear viscosities of mixtures with various PBA contents.

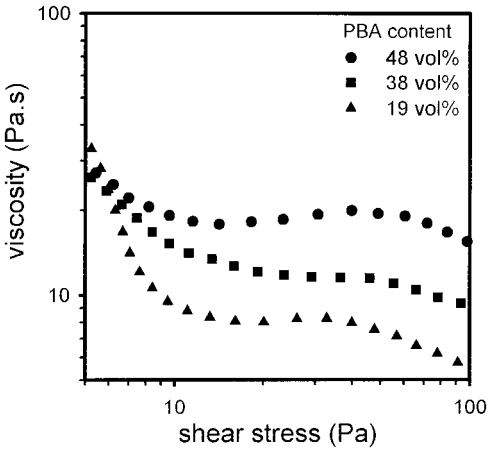

Figure 5 Shear thickening behavior of PBA/ChOC mixtures.

surements at higher shear rates were possible, the Newtonian plateau and the second shear shinning region could be observed. From Figure 3, one can easily note that the rheological behavior of ChOC containing 5% PBA is essentially analogous to that of pure ChOC. Similarly, a small amount of the ChOC suspensions does not change the Newtonian behavior inhered in the PBA matrix, as shown by the viscosity/shear rate curves for samples at 89 and 94% volume percentage.

Shown in Figure 4 are the steady viscosities of ChOC continuous phases with higher PBA content. As the PBA volume fraction increases, the shear-thinning behavior at low shear rates is preserved. Between the shear-thinning region and the Newtonian plateau at higher shear rates, a distinct shear thickening behavior appears in the intermediate rate range. A local viscosity maximum emerges in this range. As PBA volume fraction increases, height of the peak increases and the shear thickening onset shifts to a lower shear rate. Replacing the horizontal axis in Figure 4 by shear stress as shown in Figure 5, one can easily see that the shear thickening onset and the viscosity maximum location occur at approximately the same stress level for each PBA sample with different contents; the amounts of the components are irrelevant.

The composition effects on the viscosity can be seen from Figure 6, which plots the viscosity-composition curves at different stress levels. When PBA occupies a small volume fraction, a normal emulsion effect (i.e., increasing the PBA amount enhances the system viscosity) was observed. In the mid-PBA volume fraction range, a maximum on the curve occurs when the shear stress is low, and as the shear stress increases, the maximum shifts to a lower volume fraction of PBA and the height of the peak reduces. Finally, it disappears at the 200-Pa stress level. The existence of the maximum indicates that the emulsion effect is counteracted by a viscosity reduction effect, which can be clearly seen in the following. In a PBA dominant blend, addition of ChOC to PBA always causes a reduction in viscosity. At low stress levels, the viscosities of PBA-rich mixtures decrease slightly as ChOC content increases and it becomes drastic as the liquid crystal volume fraction approaches 0.5. As stress level increases, the addition of ChOC becomes more effective on the viscosity reduction.

It is well known that LCP addition induces a viscosity reduction to various blends,[21–24] and on several occasions, a viscosity minimum occurs at an appropriate composition.[12–14,25] Most of these experiments were conducted in capillaries. In investigation on extrudate morphologies, LCPs were found to assume elongated ellipsoids or fibril forms.[21–22] Migration of the dispersed LCP to high deformation rate regions

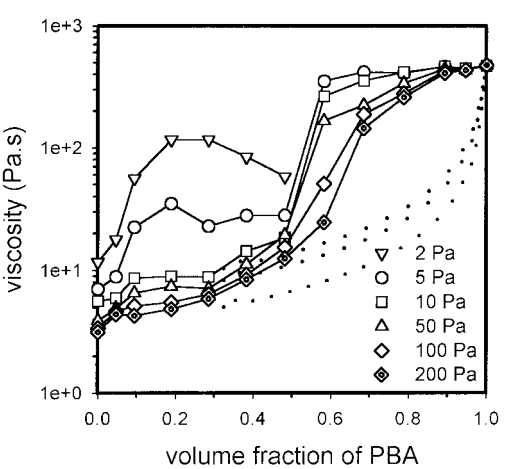

Figure 6 Viscosity as a function of volume fraction at different stress levels. The data are obtained by interpolation from data in Figures 3 and 4.

such as the neighborhood of the capillary wall forming a sheath/core morphology was also reported.[23–24] Blend viscosity reduction caused by LCP addition was attributed to the interfacial slip[26–28] or lubrication at the die wall.[29] Our measurements were performed in a homogenous flow field provided by a cone-and-plate fixture. Migration of LCP can therefore be excluded. We expected that ChOC droplets suspended in PBA would deform into elongated ellipsoids or even fibrils or filaments under the shear flow for the following reasons. The viscosity ratios of ChOC to PBA are very small, especially at higher shear rates, and the system has a rather small interfacial tension, 1.6×10^{-4} N/m. The viscosity ratios ranged from 6.7×10^{-3} to 1.5×10^{-2} depending on the magnitude of the shear stress. At such high viscosity ratios, Rumscheidt and Mason[30] showed that the droplets would assume a sigmoidal shape and smaller droplets could be shed off from two tips, if both fluids are Newtonian. Corresponding to a given shear rate, a larger-sized droplet is able to survive from breaking up and suffers a deformation which is described by the ratio of the original droplet diameter to the minimum diameter of the deformed droplet, or the reduced droplet diameter. Following the prediction by Hinch and Acrivos,[31] the reduced droplet diameter of the largest droplet could range from 7 to 10 for stress levels from 2 to 200 Pa in this system, and hence, a large deformation of the droplets in our systems is expected. Deformation could be underestimated, because the viscoelasticity of PBA could help the ChOC droplet to resist breakage, as predicted by Vonoene.[32] Larger ChOC droplets are expected to survive compared to pure viscous systems at the same shear rate, and consequently, more severe deformation could result. Moreover, the unique liquid crystallinity feature of ChOC might also enhance the filament stability to prevent them from breaking up through the varicose mechanism[33,34] because the liquid crystallinity of ChOC may play the same role as the elasticity in general polymer systems. The elasticity of nematic and chiral nematic liquid crystals originates from the director distortion. The parallel arrangement of a director field provides a minimum free energy, and naturally, is the energetically favored state. The varicose breaking-up mechanism essentially originated from the growth of a sinusoidal disturbance at the interface. An elongated ellipsoid or fibril that resembles a cylinder produces a lower director distortion-free energy than when a sinusoidal interfacial displacement fluctuation is superimposed on it. In the former, the directors can arrange themselves in parallel to the long axis of the ellipsoid or the fibrils if the tangential direction is the preferred direction of the director on the interface. In the latter, the directors must curve themselves along the sinusoidal interface, which loses parallelism and produces more director distortion. Normally, the elastic constant values for the director distortion in nematics are on the order of 10^{-11} N.[35] In our system, if the droplets are micrometer in size, the interfacial tension, which is the driving force for droplet breakup, could produce a stress order of 100 Pa. Under the same droplet size, the director distortion could produce a force order of 10 Pa. To some extent, this counteracts the interfacial tension to resist droplet breakup. Therefore, in this system, except in a few low-shear stress situations, the ChOC droplets suspended in PBA are expected to deform into extremely elongated ellipsoids or into fibrils under the shear flow. In Figure 6, one can easily see that the viscosity reduction from ChOC addition becomes more prominent as the shear stress increases. This is consistent with the above discussion, because at higher stress, ChOC droplets are more elongated. The mechanism for the viscosity reduction by formation of the fibril morphology is not clear. However, the reduction mechanism cannot be simply interpreted by using a layer structure and interfacial slip. The simple fluidity additivity rule, presented by the dotted curves in Figure 6, could describe a biphasic flow in layer morphology without interfacial slip. A prediction using this rule produces a large underestimation and a worse prediction could result if the slip is included. Because the simple additivity rule can be derived from layer morphology, this indicates that over the stress level and the concentration range we investigated, the biphasic flow never assumes such morphology. It is suggested that the fibril formation could lower the viscosity of the biphasic flow to a value that is higher than the viscosity value in layer morphology and lower than that in suspended spheroid morphology.

The reason for shear thickening is not clear. Shear thickening has been reported to occur in suspended solid particle systems[36–38] and some low-concentration surfactant systems.[39,40] Liquid–liquid biphasic systems that exhibit shear thickening have seldom been reported. The mechanisms that explain shear thickening for those systems are expected not to be feasible for this liquid–liquid system. The shear thickening mechanism for this system could be interpreted by using phase inversion. At high shear rates, the viscosity ratio of the two phases is extremely low and phase inversion could easily occur, as predicted by Paul and Barlow[41] or by Metelkina and Blekht[42]; even PBA volume fraction is as low as 0.05. At somewhat low shear rates, the phase inversion may not occur for mixtures at low PBA content, because the viscosity of ChOC is in the first shear-thinning regime, which induces higher viscosity ratio and the strength of the flow is not strong enough to trigger phase inversion. When the shear stress is higher than 10 Pa, phase inversion might occur in some portion of the flowing mixture, leading to a more viscous matrix in that portion, and hence, a higher viscosity.

CONCLUSION

The steady shear viscosities of a liquid crystal (ChOC)/polymer (PBA) system at various compositions were reported. The biphasic system shows a reduction in flow resistance with the addition of the liquid crystal to the polymer. The reduction in viscosity might relate to the transformation of the suspended phase into elongated droplets or fibril. Shear thickening occurs when the shear stress level reaches 10 Pa for mixtures with a PBA content between 10 and 50%.

References

1. Pal, R.; Rhodes, E. J Colloid Interface Sci 1985, 107, 301.
2. Newab, M. A.; Mason, S. G. Trans Faraday Soc 1958, 54, 1712.
3. Van der Waarden, M. J Colloid Sci 1954, 9, 215.
4. Eilers, H. Kolloid-Z 1943, 102, 154.
5. Schlund, B.; Ultracki, L. A. Polym Eng Sci 1987, 27, 359.
6. Dobbrescu, V.; Cobzaru, V. J Polym Sci, Polym Symp 1978, 64, 27.
7. Wang, K. J.; Lee, J. L. J Appl Polym Sci 1987, 33, 431.
8. Han, C. D.; King, R. G. J Rheol 1980, 24, 213.
9. Kim, W. N.; Denn, M. M. J Rheol 1992, 36, 1477.
10. Weiss, R. A.; Huh, W.; Nicolais, L. Polym Eng Sci 1987, 27, 684.
11. Valenza, A.; La Mantia, F. P.; Paci, M. Int Polym Proc 1991, 6, 247.
12. Siegmann, A.; Dagan, A. G.; Kenig, S. Polymer 1985, 26, 1330.
13. Kohli, A.; Chung, N.; Weiss, R. A. Polym Eng Sci 1989, 29, 573.
14. Kulichikhin, V. G.; Plate, N. A. Polym Sci (USSR) 1991, 33, 1.
15. Brandrup, J.; Immergut, E. H. Polymer Handbook, 3rd ed.; Wiley Interscience: New York, 1989.
16. Onogi, S.; Asada, T. in Rheology; Plenum Press: New York, 1980; Vol. 1, p. 127.
17. Kiss, G.; Porter, R. J. J Polym Sci, Polym Phys Ed 1980, 18, 361.
18. Pochan, J. M.; Erhardt, P. F. Phys Rev Lett 1971, 27, 790.
19. Pochan, J. M.; Marsh, D. G. J Chem Phys 1972, 57, 1193.
20. Wissbrun, K. F. J Rheol 1981, 25, 619.
21. Minkova, L. I.; De Petris, S.; Paci, M.; Magagnini, P. L. J Appl Polym Sci 1994, 52, 1653.
22. Jang, S. H.; Kim, B. S. Polym Eng Sci 1995, 35, 6
23. Siegmann, A.; Dagan, A.; Kenig, S. Polymer 1985, 26, 30.
24. Isayev, A. F.; Modic, M. Polym Comp 1987, 8, 158.
25. Blizard, K. G.; Baird, D. G. Polym Eng Sci 1987, 27, 653.
26. La Mantia, F. P.; Valenza, A.; Paci, M. Polym Eng Sci 1990, 30, 7.
27. Nobile, M. R.; Amendola, E.; Nicolais, L. Polym Eng Sci 1989, 29, 244.
28. Acierno, D.; Amendola, E.; Carfagna, C. Mol Cryst Liq Cryst Sci Technol 1987, 153, 553.
29. Collyer, A. A.; Clegg, D. W.; France, G. H. IXth Int Congr Rheol 1985, 3, 543.
30. Rumscheidt, F. D.; Mason, S. G. J Colloid Sci 1961, 16, 210.
31. Hinch, E. J.; Acrivos, A. J Fluid Mech 1980, 98, 305.
32. Vonoene, H. J Colloid Int Sci 1972, 40, 448.
33. Rayleigh, L. Proc Lond Math Soc 1879, 10, 4.
34. Tomotika, S. Proc Roy Soc 1935, 150, 322.
35. de Gennes, P. G.; Prost, J. in The Physics of Liquid Crystals, 2nd ed.; Clarendon Press: Oxford, 1993; Chapter 3.
36. Barnes, H. A. J Rheol 1989, 33, 329.
37. Hoffman, R. L. Trans Soc Rheol 1972, 16, 155.
38. Bender, J.; Wagner, N. J Rheol 1996, 40, 899.
39. Kalus, J.; Hoffmann, H.; Chen, S. H.; Linder, P. J Phys Chem 1989, 93, 4267
40. Hu, Y. T.; Wang, S. Q.; Jamieson, A. M. J Rheol 1993, 37, 531.
41. Paul, D. R.; Barlow, J. W. J Macromol Sci Rev Macromol. Chem 1980, C18, 109.
42. Metelkina, V. I.; Blekht, V. S. Kolloid Zh 1983, 46, 476.